Nonlinear Processes in Geophysics (2001) 8: 151–157

Nonlinear Processes in Geophysics

A Monte Carlo simulation of magnetic field line tracing in the solar wind

P. Pommois, G. Zimbardo, and P. Veltri

Dipartimento di Fisica, Università della Calabria, and Istituto Nazionale per la Fisica della Materia, Unità di Cosenza, I-87030 Arcavacata di Rende, Italy

Received: 6 July 2000 – Revised: 5 March 2001 – Accepted: 2 April 2001

Abstract. It is well known that the structure of magnetic field lines in solar wind can be influenced by the presence of the magnetohydrodynamic turbulence. We have developed a Monte Carlo simulation which traces the magnetic field lines in the heliosphere, including the effects of magnetic turbulence. These effects are modeled by random operators which are proportional to the square root of the magnetic field line diffusion coefficient. The modeling of the random terms is explained, in detail, in the case of numerical integration by discrete steps. Furthermore, a proper evaluation of the diffusion coefficient is obtained by a numerical simulation of transport in anisotropic magnetic turbulence. The scaling of the fluctuation level and of the correlation lengths with the distance from the Sun are also taken into account. As a consequence, plasma transport across the average magnetic field direction is obtained. An application to the propagation of energetic particles from corotating interacting regions to high heliographic latitudes is considered.

1 Introduction

If charged particles have Larmor radius much smaller than the typical turbulence scale lengths, with good approximation, they move along the magnetic field lines so that the magnetic field structure determines particle transport. In addition to the global, average magnetic field configuration, a relevant level of magnetic turbulence is often present in space plasmas, which induces a random walk of magnetic field lines (Jokipii and Parker, 1968, 1969). This problem also attracted much interest in the plasma fusion field as well (Rosenbluth et al., 1966; Rechester and Rosenbluth, 1978; Krommes et al., 1983; Isichenko, 1991).

Here, we perform a numerical study of field line transport in the presence of magnetic turbulence. In order to trace the magnetic field lines in the heliosphere, we first integrate the magnetic field lines in a local cartesian frame, where a three-dimensional model of magnetic turbulence allows us to evaluate a non quasilinear magnetic field line diffusion coefficient even in the case of anisotropic turbulence, as observed in the solar wind. Then, by means of a Monte Carlo simulation, where a random force term proportional to the diffusion coefficient is added to the magnetic field line equations, we evaluate how the magnetic field lines diffuse in the heliosphere. To this end, simple but physically based assumptions on the scaling of the fluctuation level and of the correlation lengths with the radial distance are made. Finally, we consider Ulysses' recurrent observations of energetic particles at high southern heliographic latitudes, made during its first descent toward the south polar region (e.g. Sanderson et al., 1995; Simnett et al., 1998). These particles are accelerated by corotating interaction regions (CIRs), which extend in latitude up to about $\pm 35°$, while energetic particles enhancements were observed up to 70°–74° S for protons, and even 80° S for electrons. We show that latitudinal magnetic field line diffusion due to anisotropic magnetic fluctuations can indeed explain the propagation to such southern latitudes of both ions and electrons.

2 Numerical simulation

The study is carried out in two consecutive steps: first, we perform the simulations in a local Cartesian frame (x, y, z) (see Fig. 1) to determine the influence of the magnetic turbulence on the diffusion coefficients; second, we perform a Monte Carlo simulation to consider the inhomogeneity of the heliosphere, and to take into account the solar wind magnetic spiral structure. For this second step, spherical coordinates are used. This implies a separation of scales, e.g. that the turbulence correlation length is much smaller than the radius of curvature of the spiral, so that the diffusion coefficient found in the local, Cartesian frame can be used in the global, heliospheric simulation.

The magnetic field lines are, by definition, those lines which are tangent at any point in space to the magnetic field

Correspondence to: P. Pommois (pommois@fis.unical.it)

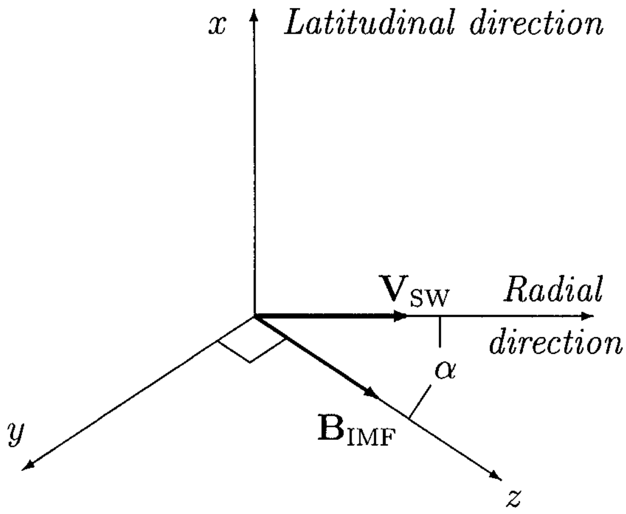

Fig. 1. Local reference frame in the solar wind.

direction. This means that the elementary displacement $d\boldsymbol{r}$ along the field line is parallel to $\boldsymbol{B}(\boldsymbol{r})$; we can express this by writing $d\boldsymbol{r} = \boldsymbol{B} d\lambda$, where $d\lambda$ is a scalar quantity. If $d\lambda$ is choosen as $ds/|\boldsymbol{B}|$, we obtain the field line equations as $d\boldsymbol{r}/ds = \boldsymbol{B}/|\boldsymbol{B}|$, and it is easily verified that ds is the arc length element along $\boldsymbol{B}$. If we choose $d\lambda$ as $d\xi/B_0$, with B_0 a constant, this yields

$$\frac{d\boldsymbol{r}}{d\xi} = \frac{\boldsymbol{B}(\boldsymbol{r})}{B_0} = \frac{\boldsymbol{B}_0 + \delta\boldsymbol{B}(\boldsymbol{r})}{B_0} \tag{1}$$

where $\boldsymbol{B}_0 = B_0\hat{\boldsymbol{e}}_z$ is the average field and $\delta\boldsymbol{B}(\boldsymbol{r})$ the fluctuating magnetic field. In this set of nonlinear, stochastic ordinary differential equations, $\boldsymbol{r} \equiv (x, y, z)$ are the unknowns, and ξ is the independent variable. It can be seen that ξ represents the length of the unperturbed field lines (the same is true if $B_0(\boldsymbol{r}) = |\boldsymbol{B}_0(\boldsymbol{r})|$ varies in space). For $\delta\boldsymbol{B} \neq 0$, the ensemble average of $d\boldsymbol{r}/d\xi$ yields ξ as the average value of the projection of field lines on the unperturbed field $\boldsymbol{B}_0$, i.e. $d\xi = \langle d\boldsymbol{r} \cdot \boldsymbol{B}_0/B_0\rangle = \langle d\boldsymbol{r} \cdot \hat{\boldsymbol{e}}_z\rangle = \langle dz\rangle$. We choose this form of the field line equations as it is more appropriate to perform the Monte Carlo simulation reported below.

2.1 Diffusion coefficients in local anisotropic turbulence

Here, as a first step, we evaluate the diffusion coefficients of magnetic field lines in an anisotropic magnetic turbulence. We assume the local frame (x, y, z) of Fig. 1, and use the Cartesian geometry. Such a local approach is justified by the fact that the correlation length of the magnetic turbulence is much smaller than the scale of variation of the average spiral field (to be discussed later).

Magnetic turbulence is represented as the sum of static magnetic perturbations (Pommois et al., 1999a; Zimbardo et al., 2000):

$$\delta\boldsymbol{B}(\boldsymbol{r}) = \sum_{\boldsymbol{k},\sigma} \delta B(\boldsymbol{k})\hat{\boldsymbol{e}}_\sigma(\boldsymbol{k}) \exp i[\boldsymbol{k}\cdot\boldsymbol{r} + \phi_{\boldsymbol{k}}^\sigma] \tag{2}$$

where $\hat{\boldsymbol{e}}_\sigma(\boldsymbol{k})$ are the polarization unit vectors, $\phi_{\boldsymbol{k}}^\sigma$ are random phases, and the Fourier amplitude $\delta B(\boldsymbol{k})$ is given by the spectrum:

$$\delta B(\boldsymbol{k}) \propto \frac{1}{({k_x}^2{l_x}^2 + {k_y}^2{l_y}^2 + {k_z}^2{l_z}^2)^{\gamma/4+1/2}} \tag{3}$$

where $\gamma = 3/2$ is the spectral index, and l_x, l_y, l_z are the correlation lengths in the x, y, and z directions, respectively. Different values of the correlation lengths quantify the anisotropy of turbulence as they define the shape of the ellipsoid representing the excited wave mode distribution in $\boldsymbol{k}$–space.

By integrating a large number N of magnetic field lines with different initial conditions, the variances

$$\langle \Delta {x_i}^2\rangle = \frac{1}{N}\sum_{j=1}^{N}\left[x_{i,j}(\xi) - x_{i,j}(0)\right]^2 \tag{4}$$

can be computed as a function of the integration parameter ξ, and the diffusion coefficients are obtained from the transport law $\langle \Delta {x_i}^2\rangle = 2D_i\xi$ $(i = x, y)$. (See Zimbardo et al., 1995; Pommois et al., 1998, 1999a, for more details on the numerical technique).

Extensive numerical simulations of magnetic field line transport were performed with a similar model by Pommois et al. (1999a) in the case of anisotropy in the plane perpendicular to the average field $\boldsymbol{B}_0$, and by Zimbardo et al. (2000) in the case of anisotropy axially symmetric around $\boldsymbol{B}_0$. We have computed the diffusion coefficient in the more general case when all the correlation lengths are different, as a function of $\delta B/B_0$, and where l_z/l_y equals either 1 or 10, and l_x/l_y varies from 1 to 8. Such a range of correlation lengths is consistent with that found from the analysis of the solar wind data (Matthaeus et al., 1990; Carbone et al., 1995). Indeed, several studies of solar wind turbulence indicate a strong anisotropy in the correlation lengths, although further data analysis is needed to better constrain the values of l_x, l_y, and l_z. Note that the anisotropy of turbulence has been studied also considering a two-component model, i.e. two-dimensional plus slab fluctuations (Matthaeus et al., 1995; Gray et al., 1996), which implies very strong anisotropy, axially symmetric around $\boldsymbol{B}_0$. Indeed, the slab component corresponds to $l_z \ll l_x, l_y$, while the two-dimensional component corresponds to the limit $l_z \gg l_x, l_y$. However, for this study, we maintain a single component anisotropic model which can reproduce either the slab or the two-dimensional model (see Zimbardo et al., 2000).

For the fluctuation levels relevant to the solar wind, $\delta B/B_0 \simeq 0.5$–1 (e.g. Zank et al., 1998), and for the degrees of anisotropy of interest, the diffusion coefficients obtained by numerical simulation can be modelled by the following simple expression (Pommois et al., 2001):

$$D_i = \mathcal{D}\left(\frac{\delta B}{B_0}\frac{l_z}{l_x}\right)^{\mu}\frac{l_x}{l_z}\left(\frac{l_i}{l_x}\right)^{\nu} l_x \tag{5}$$

with $i = x, y$, and where $\mathcal{D}$, μ and ν are dimensionless parameters. Note that the field line diffusion coefficient D_i

has the dimensions of a length. In the above expression, the "spare" l_x is to be used to set the physical value of D_i. A best fit of the computed diffusion coefficient yields $\mathcal{D} = 0.028$, $\mu = 1.51$ and $\nu = 0.67$. The best fitting line is shown in Fig. 2, together with the diffusion coefficients. In order to appreciate the scaling of D_i with the fluctuation level, we plotted $D_i/[(l_x{}^2/l_z)(l_i/l_x)^\nu]$ versus $(\delta B/B_0)(l_z/l_x)$. As can be seen, a scaling of D_i different from the quasilinear one (which implies $\mu = 2$) is obtained (see also Gray et al., 1996). Equation (5) implies that if $l_x > l_y$, then $D_x > D_y$, as well, and this anisotropy is often found in the solar wind ($l_x > l_y$) (Carbone et al., 1995), where the x direction is chosen according to Fig. 1.

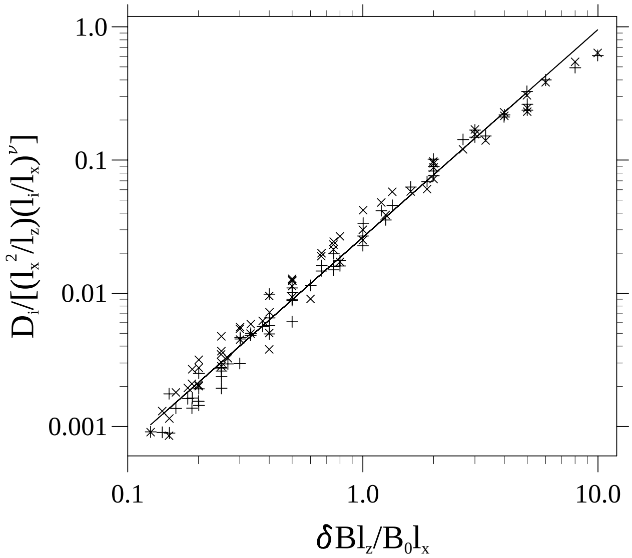

Fig. 2. Ratio $D_i/[(l_x{}^2/l_z)(l_i/l_x)^\nu]$ versus $(\delta B/B_0)(l_z/l_x)$ and best fitting line for these data. Markers: Plus signs for D_x; crosses for D_y.

2.2 Monte Carlo simulation of field line tracing

As a second step, we trace the magnetic field lines in the heliosphere by integrating Eq. (1) and taking into account that the average magnetic field $\boldsymbol{B}_0(\boldsymbol{r})$ corresponds to the usual solar wind field (Parker, 1958). In spherical coordinates, we have

$$\begin{aligned} \langle B_r \rangle &= B_{r\mathrm{E}} \left(\frac{r_\mathrm{E}}{r}\right)^2 \\ \langle B_\vartheta \rangle &= 0 \\ \langle B_\varphi \rangle &= -B_{r\mathrm{E}} \left(\frac{r_\mathrm{E}}{r}\right)^2 \frac{\Omega\, r}{V_\mathrm{SW}} \cos\vartheta \end{aligned} \quad (6)$$

where r is the radial distance from the Sun, ϑ is the heliographic latitude, φ is the longitude, $B_{r\mathrm{E}}$ is the radial component of the solar wind magnetic field at the Earth ($r_\mathrm{E} = 1$ AU) and Ω is the solar rotation rate (26 days). In order to take into account the fast and slow stream structure of the solar wind, the solar wind speed is modeled as

$$V_\mathrm{SW} = V_\mathrm{max} - \frac{V_\mathrm{max} - V_\mathrm{min}}{1 + (\sin\vartheta/\sin\vartheta_t)^8} \quad (7)$$

where $V_\mathrm{max} = 750$ km/s, $V_\mathrm{min} = 350$ km/s, and the transition velocity latitude is $\vartheta_t = 15°$ (e.g. Kóta and Jokipii, 1995).

The fluctuating magnetic field component is now modeled as a random process, i.e. $\delta\boldsymbol{B}(\boldsymbol{r})/B_0(\boldsymbol{r})$ in Eq. (1) is replaced by (Kubo et al., 1985; Binder, 1979)

$$\frac{\delta B_i(\boldsymbol{r})}{B_0(\boldsymbol{r})} = \eta_i(\xi) A_i(\boldsymbol{r}) \quad (8)$$

where $i = x, y$ in the local frame of reference of Fig. 1, and $\eta_x(\xi)$ and $\eta_y(\xi)$ are two uncorrelated random functions with no memory (white noise) (Uhlenbeck and Ornstein, 1930). It should be understood that Eq. (8) leads to the same average field lines and the same transport properties of Eq. (1), but the random term $\eta_i(\xi)A_i(\boldsymbol{r})$ is not meant to represent a realization of the fluctuating magnetic field. Indeed, the diffusion properties of Eq. (1) were studied in the previous subsection, and the value of the diffusion coefficients, Eq. (5), is now used to assess the amplitude of $A_i(\boldsymbol{r})$, as indicated below. Indeed, it is straightforward to show that Eq. (8) leads to a transport law of the form $\langle \Delta r^2 \rangle = 2D\xi$. In the case of analytic integration of Eqs. (1) and (8), the random "force" amplitudes $A_i(\boldsymbol{r})$ are related to the diffusion coefficients in Eq. (5) by $A_i(\boldsymbol{r}) = \sqrt{6D_i(\boldsymbol{r})}$ (Uhlenbeck and Ornstein, 1930; Veltri et al., 1990).

It is interesting to notice that when performing numerical integration by discrete steps, $\Delta\xi$, the relation between $A_i(\boldsymbol{r})$ and $D_i(\boldsymbol{r})$, is somewhat modified. In the discrete case, η_i is a dimensionless random number evenly distributed between -1 and $+1$. We number by n the integration steps, whose total number we call M and integrate Eqs. (1) and (8) in a direction perpendicular to the average field, for example, the x component. Then $\Delta x_n/\Delta\xi_n = \eta_x(\xi_n)A_x(\boldsymbol{r})$, if we consider equal steps $\Delta\xi$, yields,

$$(\Delta x)_M = \Delta\xi \sum_{n=1}^{M} \eta_x(\xi_n) A_x(\boldsymbol{r}_n) \quad (9)$$

Upon squaring we obtain

$$(\Delta x)_M^2 = (\Delta\xi)^2 \sum_{n=1}^{M}\sum_{m=1}^{M} \eta_x(\xi_n)\eta_x(\xi_m) A_x(\boldsymbol{r}_n) A_x(\boldsymbol{r}_m) \quad (10)$$

The random numbers are δ–correlated, and that corresponds to $\langle \eta_x(m)\eta_x(n)\rangle = \delta_{nm}/3$, therefore,

$$\langle (\Delta x)_M^2 \rangle = \frac{(\Delta\xi)^2}{3} \sum_{n=1}^{M} A_x(\boldsymbol{r}_n) A_x(\boldsymbol{r}_n) \quad (11)$$

Now we make use of the assumption of separation of scales as given above, i.e. the correlation length of the turbulence (the diffusion scale) has to be much smaller than the radial scale of change of the averaged quantities, which is the heliocentric distance r. Thus, the quantity $A_x(\boldsymbol{r}_n)A_x(\boldsymbol{r}_n)$ can be taken out of the sum and we have M equal addends, yielding

$$\langle (\Delta x)_M^2 \rangle = \frac{A_x{}^2(\boldsymbol{r}_n)}{3} M(\Delta\xi)^2 \quad (12)$$

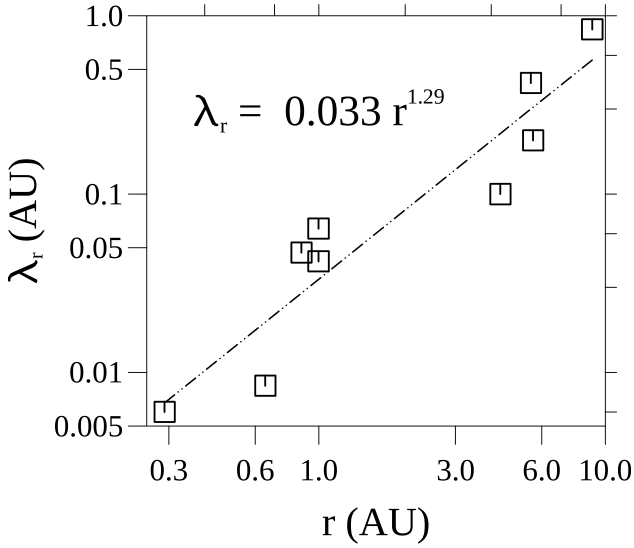

Fig. 3. Breakpoint wavelength versus radial distance (open squares). Best fitting line (dash-dotted line). From Pommois et al. (1999b).

The total number of steps M is related to the total displacement ξ along the unperturbed field lines by $M = \xi/\Delta\xi$, whence

$$\langle(\Delta x)_M{}^2\rangle \equiv \langle(\Delta x)_\xi{}^2\rangle = \frac{A_x{}^2(\boldsymbol{r})}{3}\xi\Delta\xi \tag{13}$$

Comparison of this expression with the standard diffusion law shows that in the case of numerical integration by discrete steps the random "kick" amplitude $A_x(\boldsymbol{r})$ must be related to the diffusion coefficient by

$$A_x = \sqrt{\frac{6D_x}{\Delta\xi}} \tag{14}$$

A similar expression for A_y is obtained. It can be seen that A_x is dimensionless, since both D_x and $\Delta\xi$ have the dimensions of a length, and that A_x depends on the value of the integration step $\Delta\xi$. In practice, at each step in the numerical integration, the field line position $\boldsymbol{r}$ is advanced along the unperturbed field by $\Delta\xi$, and perpendicular to the unperturbed field by $\eta_x A_x \Delta\xi = \eta_x\sqrt{6D_x\Delta\xi}$. Also, note that the standard estimate of diffusion coefficients as the mean square displacement λ^2 over the displacement time τ, $D \sim \lambda^2/\tau$, is recovered from the above expression when $\lambda \to \eta A_x \Delta\xi$ and $\tau \to \Delta\xi$.

2.3 Expression of the diffusion coefficient in the solar wind

In order to have the numerical value of the diffusion coefficients in Eq. (5), it is necessary to relate l_x to the correlation lengths of the observed magnetic turbulence. Introducing the radial correlation length λ_r and the angle α between the average magnetic field and the radial direction (see Fig. 1), we obtain that the expression of l_x is

$$l_x = \lambda_r\left(\frac{l_y{}^2}{l_x{}^2}\sin^2\alpha + \frac{l_z{}^2}{l_x{}^2}\cos^2\alpha\right)^{-1/2} \tag{15}$$

Using the data on magnetic turbulence of several spacecrafts, Horbury et al. (1996) reported the value of the radial breakpoint wavenumber k_r as a function of r. The breakpoint wavenumber corresponds to the change of slope in the magnetic fluctuation spectrum, and marks the beginning of the inertial range of turbulence. The corresponding breakpoint wavelength represents the radial correlation length. A best fit of $\lambda_r = 2\pi/k_r$ as a function of the distance from the Sun yields (see Fig. 3)

$$\lambda_r(r) = \left(\frac{r}{r_\mathrm{E}}\right)^{1.29} \times 0.033\mathrm{AU} \tag{16}$$

Next, the variation of the turbulence level $\delta B/B_0$ as a function of the position $\boldsymbol{r}$ of the magnetic field lines is to be considered, as well. The magnetic fluctuations δB are assumed to evolve with radial distance according to the WKB scaling, i.e. $\delta B^2/\delta B_\mathrm{E}{}^2 \sim r_\mathrm{E}{}^3/r^3$, where δB_E is the fluctuation amplitude at the Earth's orbit. The WKB scaling of magnetic fluctuations in the solar wind has been confirmed for turbulence periods less than 2 hours and at 10 hours by Belcher and Burchsted (1974), and by Roberts et al. (1990), respectively, and for periods up to one day by Jokipii et al. (1995) and Goldstein et al. (1995), out of the ecliptic plane. At larger scales a slower decay with distance is found by Jokipii et al. (1995), although Goldstein et al. (1995) report indications of the WKB scaling down to 10^{-6} Hz. While understanding the scaling of magnetic turbulence with distance is a basic issue for solar wind studies (e.g. Zank et al., 1996), we adopt the WKB scaling as a simple model consistent with observations. On the other hand, the slower decay of the fluctuations at larger scales would enhance the field line transport reported below. Thus, the magnetic turbulence level is modelled as

$$\frac{\delta B}{B_0} = \frac{\delta B_\mathrm{E}}{B_\mathrm{E}}\left(\frac{1+\beta^2 r_\mathrm{E}{}^2}{1+\beta^2 r^2\cos^2\vartheta}\right)^{1/2}\left(\frac{r}{r_\mathrm{E}}\right)^{1/2} \tag{17}$$

where $\delta B_\mathrm{E}/B_\mathrm{E}$ is the fluctuation level at 1 AU in the ecliptic plane (here, $B_\mathrm{E} = B_{r\mathrm{E}}\left(1+\beta^2 r_\mathrm{E}{}^2\right)^{1/2}$ and $\beta = \Omega/V_\mathrm{SW}$). Finally, the value of the diffusion coefficient $D_i(\boldsymbol{r})$ to be used for modelling the random "force" in Eq. (14), is obtained by inserting Eqs. (15) and (17) into Eq. (5).

3 Results of the simulation

In the simulation, we fix the starting point of the magnetic field line at $(r_0, \vartheta_0, \varphi_0)$, and we choose the parameters modelling the fluctuations, i.e. $\delta B_\mathrm{E}/B_\mathrm{E}$, l_y/l_x and l_z/l_x. For instance, for an anisotropy of the correlation lengths given by $l_x/l_y = l_x/l_z = 8$, a fluctuation level at 1 AU of $\delta B_\mathrm{E}/B_\mathrm{E} = 0.7$ (Zank et al., 1998), and an assumed source of energetic

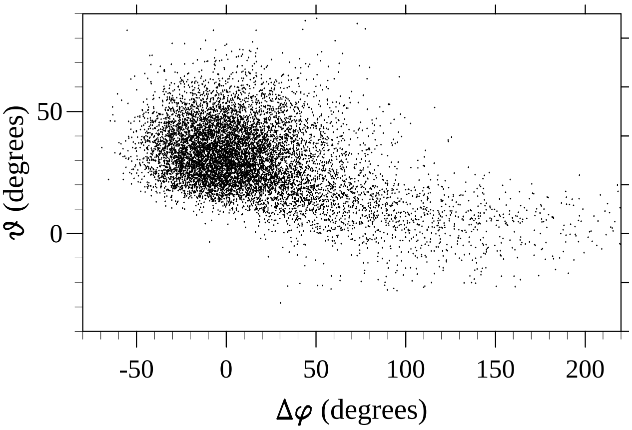

Fig. 4. Values of the angle ϑ and $\Delta\varphi = \varphi - \varphi_0$ obtained at the end of the integration for 10000 lines (see text).

particle on field lines corresponding to $r_0 = 8$ AU and to $\vartheta_0 = 30° \pm 10°$, we show in Fig. 4 the angular distribution of field lines obtained at an heliocentric distance of $r = 3$ AU. Note that the spread in azimuth at low latitudes (i.e. the "tail" in Fig. 4) is due to the change of the solar wind velocity at $\vartheta_t = 15°$ of latitude (for more details see Pommois et al., 2000).

As an application, we consider the recurrent energetic particle events detected at high southern latitudes (70°–74°) by the Ulysses spacecraft (Simnett et al., 1998). These particles are accelerated by corotating interaction regions (CIRs) located at lower latitude (less that 35°). Ulysses also confirmed that the average magnetic field in the solar wind follows the constant latitude Parker model, even at high latitudes (Forsyth et al., 1996). Consequently, the particles accelerated at the CIR should undergo cross field transport in latitude up to 40° to be observed by Ulysses (see Fig. 5). This discovery has stimulated theorical studies on the non radial structure of the average, large scale magnetic field (Fisk, 1996), as well as studies of latitudinal diffusion due to magnetic field fluctuations (Kóta and Jokipii, 1995, 1998; Giacalone, 1999). In particular, Kóta and Jokipii (1995, 1998) have pointed out the importance of anisotropic magnetic field line diffusion.

To understand whether the magnetic turbulence can allow the propagation of the particles to high heliographic latitudes, we assume that the energetic particles are accelerated at $8 \div 10$ AU from the Sun, and we follow the magnetic field lines toward the Sun. We analyse the simulation results from the spacecraft's point of view. It is as if the pattern in Fig. 4 rotates over Ulysses every 26 days, while the spacecraft slowly changes latitude. For a given interval $\Delta\vartheta$ corresponding to the Ulysses position, we count the number of field lines in Fig. 4 as a function of φ, with $\Delta\varphi$ bins of 9°, so that we have an histogram as a function of φ. Because of the correspondence between the time and azimuthal angles, the histogram is plotted as a function of time, and when φ has increased by 360°, a new interval $\Delta\vartheta$ is considered (see

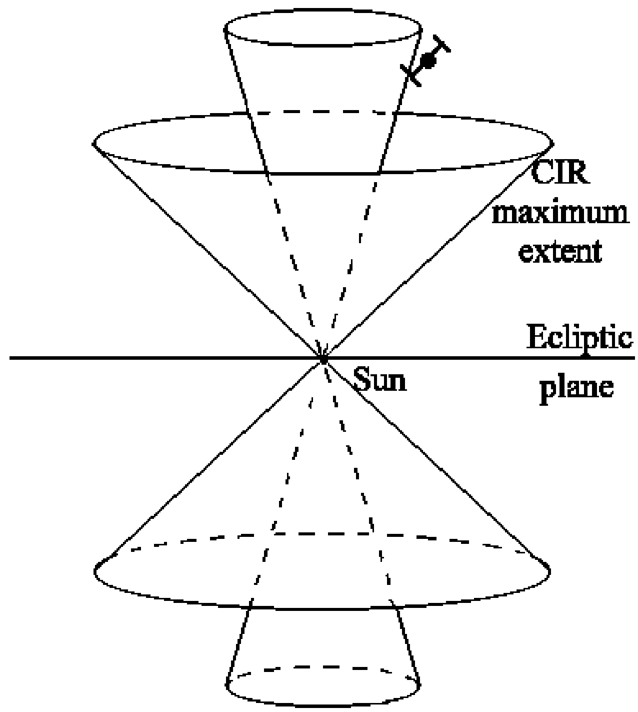

Fig. 5. Constant latitude cones indicating the zones which are connected magnetically in the solar wind. The wide cone corresponds to the maximum extent of the CIR, the narrow cone to the latitude at which Ulysses still detected recurrent energetic particles.

Pommois et al., 2000). This yields the histograms of field line distribution as a function of day of the year 1994 as reported in Fig. 6, where the ratio l_x/l_y is going from 1 to 8. It can be seen that some field lines travel until a latitude of 70° or more, and therefore show that magnetic field line diffusion can provide the required magnetic connection between CIRs and high heliographic latitudes. Increasing the anisotropy l_x/l_y leads to peaks at higher latitudes (see the variation of the high latitude peaks from top panels to bottom panels in Fig. 6). Even for a moderate degree of anisotropy, such as $l_x/l_y = 3$, there is a peak in field line distribution at $\sim 74°$ (see Fig. 6b) which is in agreement with Ulysses observations of 1 Mev protons. Increasing the distance r_0 has the same effect of increasing the fluctuation level $\delta B_E/B_E$, as shown by Fig. 6, panel (c) and (e).

It appears that when reasonable levels of anisotropy, $l_x/l_y = 3$–5, are considered, the results of the simulation of Fig. 6 (see panels b, c, e), are similar to the observations of energetic particles events made by Ulysses, and reported, for instance, by Simnett et al. (1998).

4 Conclusions

In this paper, we have presented a numerical simulation that traces the magnetic field lines in the heliosphere including the effect of magnetic turbulence. Anisotropy of turbulence is taken into account by a first numerical simulation in Carte-

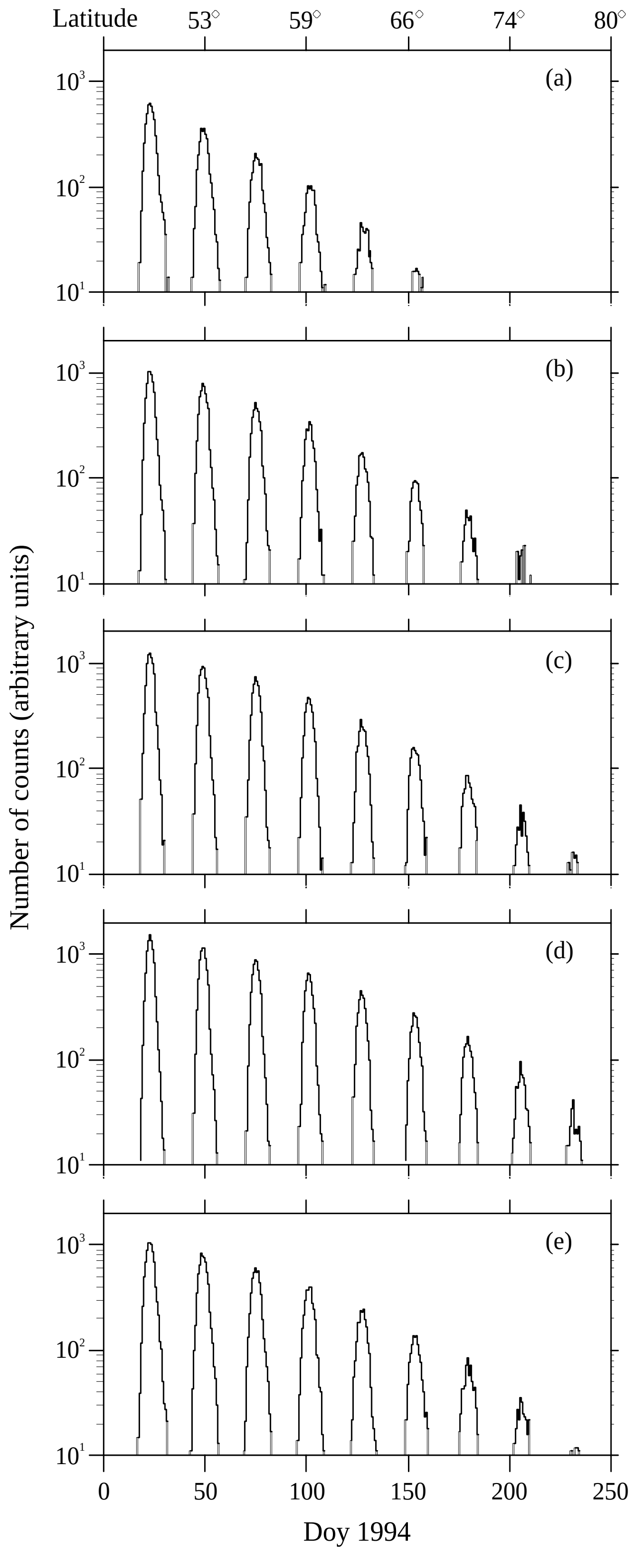

Fig. 6. Histograms of the distributions of magnetic field lines versus time obtained using the result of the Monte Carlo simulation. The lower horizontal axis reports the day of the year 1994 (see text). The simulation parameters for each run are the following: for panels **(a)**, **(b)**, **(c)** and **(d)**, $\delta B_E/B_E = 0.7$, $r_0 = 8$ AU, and **(a)**: $l_x/l_y = 1$; **(b)**: $l_x/l_y = 3$; **(c)**: $l_x/l_y = 5$; **(d)**: $l_x/l_y = 8$. For panel **(e)** $l_x/l_y = 5$, $\delta B_E/B_E = 0.5$, and $r_0 = 10$ AU.

sian geometry which leads to a proper diffusion coefficient which depends on the turbulence correlation lengths. A Monte Carlo simulation is then used to trace the magnetic field line in the heliosphere, with the representation of the random terms explained in detail. The variation of the relevant parameters with heliosphere distance is also taken into account.

We argue that diffusive field line transport can explain both the electron and the ion observations at high souther latitudes made by Ulysses (Simnett et al., 1998). Indeed, Figs. 6 exhibits peaks decreasing in intensity with latitude, with a peak at nearly 80°, as observed for the electrons.

Finally, this numerical tool can be used to study several other problems, such as the propagation of pick-up ions in the heliosphere, high latitude cosmic ray modulation by CIRs, and the propagation of solar energetic particles from the Sun to the Earth (Zimbardo et al., 2001). For these problems, other effects such as the dependence of transport on particle energy and drift motion effects are to be taken into account.

Acknowledgements. This work is supported by the Consiglio Nazionale delle Ricerche (CNR), contracts no. 98.00129.CT02, and no. 98.00148.CT02, the Ministero dell'Università e della Ricerca Scientifica e Tecnologica (MURST), the Agenzia Spaziale Italiana (ASI), contract no. ARS98-82, and the INTAS Open 97-1612 grant.

References

Belcher, J. W. and Burchsted, R., Energy densities of Alfvén waves between 0.7 and 1.6 AU, J. Geophys. Res., 79, 4765, 1974.

Binder K., Monte Carlo Methods in Statistical Physics, Springer, New York, 1979.

Carbone, V., Malara, F., and Veltri, P., A model for the three-dimensional magnetic field correlation spectra of low-frequency solar wind fluctuations during Alfvénic periods, J. Geophys. Res., 100, 1763–1778, 1995.

Fisk, L. A., Motion of the footpoints of heliospheric magnetic field lines at the sun: Implications for recurrent energetic particle events at high heliographic latitudes, J. Geophys. Res., 101 (A7), 15547–15553, 1996.

Forsyth, R. J., Balogh, A., Smith, E. J., Erdös, G., and McComas, D. J., The underlying Parker spiral structure in the Ulysses magnetic field observations, 1990–1994, J. Geophys. Res., 101, 395–403, 1996.

Gray, P. C., Pontius, D. H., and Matthaeus, W. H., Scaling of field-line random walk in model Solar Wind fluctuation, Geophys. Res. Lett., 23 (9), 965–968, 1996.

Giacalone, J., Particle transport and acceleration at corotating interaction regions, Adv. Space Res., 23, 581–590, 1999.

Goldstein, B. E., Smith, E. J., Balogh, A. et al., Properties of magnetohydrodynamic turbulence in the solar wind as observed by Ulysses at high heliographic latitude, Geophys. Res. Lett., 22, 3393–3396, 1995.

Horbury, T. S., Balogh, A., Forsyth, R. J., and Smith, E. J., The rate of turbulent evolution over the Sun's poles, Astron. Astrophys., 316, 333–341, 1996.

Isichenko, M. B., Effective plasma heat conductivity in a "braided" magnetic field - I. Quasi-linear limit, Plasma Phys. Control. Fusion, 33 (7), 795–807, 1991.

Jokipii, J. R. and Parker, E. N., Random walk of magnetic lines of force in astrophysics, Phys. Rev. Lett., 21, 44–47, 1968.

Jokipii, J. R. and Parker, E. N., Stochastic aspects of magnetic lines of force with application to cosmic-ray propagation, Astrophys. J., 155, 777–799, 1969.

Jokipii, J. R., Kóta, J., Giacalone, J. et al., Interpretation and consequences of large-scale magnetic variances observed at high heliographic latitude, Geophys. Res. Lett., 22, 3385–3388, 1995.

Kóta, J. and Jokipii, J. R., Corotating variations of cosmic rays near the south heliospheric pole, Science, 268, 1024–1025, 1995.

Kóta, J. and Jokipii, J. R., Modeling of 3–D corotating cosmic rays structures in the heliosphere, Space Sci. Rev., 83, 137–145, 1998.

Krommes, J. A., Oberman, C., and Kleva, R. G., Plasma transport in stochastic magnetic fields. Part 3. Kinetics of test particle diffusion, J. Plasma Phys., 30, 11–56, 1983.

Kubo, R., Toda, M., Hashitsume, N., Statistical Physic II: Nonequilibrium Statistical Mechanics, Springer-Verlag, Berlin, Heidelberg, 1985.

Matthaeus, W. H., Goldstein, M. L., Roberts, D. A., Evidence for the presence of quasi-two-dimensional nearly incompressible fluctuation in Solar Wind, J. Geophys. Res., 95, 20673–20683, 1990.

Matthaeus, W. H., Gray, P. C., Pontius, Jr., D. H., and Bieber J. W., Spatial structure and field-line diffusion in transverse magnetic turbulence, Phys. Rev. Lett., 75, 2136–2139, 1995.

Parker, E. N., Dynamics of the interplanetary gas and magnetic field, Astrophys. J., 128, 664–676, 1958.

Pommois, P., Zimbardo, G., and Veltri, P., Magnetic field line transport in three dimensional turbulence: Lévy random walk and spectrum models, Phys. Plasmas, 5, 1288–1297, 1998.

Pommois, P., Veltri, P., and Zimbardo, G., Anomalous and Gaussian transport regimes in anisotropic 3-D magnetic turbulence, Phys. Rev. E, 59, 2244–2252, 1999a.

Pommois, P., Veltri, P., and Zimbardo, G., Transport of magnetic field lines in the solar wind magnetic turbulence and influence on particle propagation to high heliographic latitudes, Proceedings of 9th European Meeting on Solar Physics, Magnetic Fields and Solar Processes, ESA SP-448, 1115, 1999b.

Pommois, P., Veltri, P., and Zimbardo, G., Field line diffusion in the solar wind magnetic turbulence and energetic particle propagation across heliographic latitudes, J. Geophys. Res., in press 2001.

Pommois, P., Veltri, P., and Zimbardo, G., Kubo number and magnetic field line diffusion coefficient for anisotropic magnetic turbulence, Phys. Rev. E, in press 2001.

Rosenbluth, M. N., Sagdeev, R. Z., Taylor, G. B., and Zaslavsky, G. M., Destruction of magnetic surfaces by magnetic field irregularities, Nucl. Fusion, 6, 297–300, 1966.

Rechester, A. B. and Rosenbluth, M. N., Electron heat transport in a Tokamak with destroyed magnetic surfaces, Phys. Rev. Lett., 40, 38–41, 1978.

Roberts, D. A., Goldstein, M. L., and Klein, L. W., The amplitudes of interplanetary fluctuations: stream structure, heliocentric distance, and frequency dependence, J. Geophys. Res., 95, 4203, 1990.

Sanderson, T. R., Bothmer, V., Marsden, R. G. et al., The Ulysses south polar pass: Energetic ion observations, Geophys. Res. Lett., 22 (23), 3357–3360, 1995.

Simnett, G. M., Kunow, H., Flückiger, E. et al., Corotating particle events, Space Sci. Rev., 83, 215–257, 1998.

Uhlenbeck, G. E. and Ornstein, L. S., On the theory of the Brownian motion, Phys. Rev., 36, 823–841, 1930.

Veltri, P., Mangeney, A., Scudder, J. D., Electron heating in quasi-perpendicular shocks: a Monte Carlo simulation, J. Geophys. Res., 95, 14939, 1990.

Zank, G. P., Matthaeus, W. H., and Smith, C. W., Evolution of turbulent magnetic fluctuation power with heliospheric distance, J. Geophys. Res., 101, 17093–17107, 1996.

Zank, G. P., Matthaeus, W. H., and Bieber, J. W., The radial and latitudinal dependence of the cosmic ray diffusion tensor in the heliosphere, J. Geophys. Res., 103, 2085–2097, 1998.

Zimbardo, G., Veltri, P., Basile, G., and Principato, S., Anomalous diffusion and Lévy random walk of magnetic field lines in three dimensional turbulence, Phys. Plasmas, 2, 2653–2663, 1995.

Zimbardo, G., Veltri, P., and Pommois, P., Anomalous, quasilinear, and percolative regimes for magnetic-field-line transport in axially symmetric turbulence, Phys. Rev. E, 61, 1940–1948, 2000.

Zimbardo, G., Pommois, P., and Veltri, P., Predictions for the propagation of energetic particles from the Sun to the Earth: Influence of the magnetic turbulence, Phys. Chemistry Earth, in press 2001.